scientific reports

Check for updates

OPEN

Newly-diagnosed rheumatoid arthritis patients have elevated levels of plasma extracellular vesicles with protein cargo altered towards inflammatory processes

Anne Rydland[1,2,3]✉, Fatima Heinicke[1,3,4], Tuula A. Nyman[5], Anne-Marie Siebke Trøseid[6], Siri T. Flåm[1,3], Maria Stensland[5], Johanna Gehin[7], Joakim Eikeland[7], Reidun Øvstebø[6], Maria Dahl Mjaavatten[3,8] & Benedicte A. Lie[1,2,3,5]✉

Extracellular vesicles (EVs) are implicated in rheumatoid arthritis (RA) but have mainly been assessed in RA patients taking disease modifying anti-rheumatic drugs. EVs are nanoparticles important in cell-cell communication and their molecular cargo are biomarker candidates. We characterized the protein profiles of EVs from blood plasma from newly diagnosed, treatment naïve RA patients (*N* = 32) and compared them to healthy controls (*N* = 20), by size exclusion chromatography-based EV enrichment coupled with high-resolution quantitative proteomics. The RA patients had higher EV concentration and larger EVs than controls. A total of 682 EV proteins were reliably quantified, and the overall profiles were distinctly different between patients and controls. Specifically, 26 proteins were significantly upregulated and 31 downregulated in RA patients, with several proteins acting in inflammatory networks and with immunologically important upstream regulators. The RA associated EVs appear, based on the tissue expression of their cargo proteins, to originate mainly from hepatocytes or immune cells, like neutrophils. Interestingly, the strongest RA associated EV proteins were inflammatory molecules, like SAA1 and S100A9, already suggested as biomarkers in RA. Furthermore, the RA associated EV proteins were generally not correlated with total serum protein levels, stressing the importance of EV transport of inflammatory proteins in RA pathogenesis.

Keywords Extracellular vesicles, Rheumatoid arthritis, DMARD Naïve, Inflammatory markers

Rheumatoid arthritis (RA) is a systemic autoimmune disease that predominantly affects joints, causing pannus formation, bone erosion and joint destruction. Furthermore, systemic inflammation can affect organs such as the heart, kidneys, lungs and nervous system[1–3]. RA pathogenesis encompasses close interaction between a variety of immune cells and soluble factors including cytokines, immune complexes and autoantibodies. This interaction occurs both locally in the joint but also in the circulatory system[4,5]. Rheumatoid factor (RF) and anti-citrullinated protein antibodies (ACPA) are used as diagnostic and prognostic factors[6], but despite their high specificity they have low sensitivity[7]. Hence, discovery of novel biomarkers is essential to enhance clinical care and patient outcomes.

One potential biomarker could be extracellular vesicles (EVs) that play an important role in cell-cell communication by transferring biological signals, such as nucleic acids, lipids and proteins, both locally and to

[1]Department of Medical Genetics, University of Oslo and Oslo University Hospital, Postboks 4956 Nydalen, OUS HF Ullevål sykehus, 0424 Oslo, Norway. [2]Institute of Clinical Medicine, University of Oslo, Oslo, Norway. [3]Center for Treatment of Rheumatic and Musculoskeletal Diseases (REMEDY), Diakonhjemmet Hospital, Oslo, Norway. [4]Department of Biostatistics, Institute of Basic Medical Sciences, Oslo Centre for Biostatistics and Epidemiology, University of Oslo, Oslo, Norway. [5]Department of Immunology, University of Oslo and Oslo University Hospital, Oslo, Norway. [6]The Blood Cell Research Group, Department of Medical Biochemistry, Oslo University Hospital, Ullevål, Oslo, Norway. [7]Department of Medical Biochemistry, Oslo University Hospital, Oslo, Norway. [8]Division of Rheumatology, Diakonhjemmet Hospital, Oslo, Norway. ✉email: anne.rydland@medisin.uio.no; b.a.lie@medisin.uio.no

distant parts of the body[8]. EV proteins can be located in the EV lumen, enclosed in their membrane and bound to their surface[9]. Studies on EVs derived from RA synovial fluid and plasma have revealed disease associated EV proteins such as citrullinated proteins[10–12], monocyte differentiation antigen CD14, lipopolysaccharide-binding protein, serum amyloid P-component, tenacin and cartilage oligomeric matrix protein[13] with the potential to modulate inflammatory and immunological processes. EV proteins from synovial fluid have also shown an overrepresentation of neutrophil and fibroblast markers[11]. Furthermore, plasma EVs derived from seropositive RA patients induce proinflammatory cytokine production by mononuclear phagocytes in vitro[10]. Although, an implication of EVs in RA pathogenesis is established, most studies include patients who have undergone treatment with disease modifying anti-rheumatic drugs (DMARDs). Hence, studies assessing the EV profile of treatment naïve RA patients are needed to give insights into the pathophysiology of the disease.

In this study, we investigated plasma EVs of treatment naïve, seropositive RA patients compared to age, gender and body mass index (BMI) matched healthy controls. First, we quantified and characterized the EVs, and then performed extensive high-resolution proteomics analysis coupled with bioinformatics to examine their involvement in RA.

Results

Clinical information of the study participants

All RA patients included in this study were ACPA positive and DMARD naïve, and there were no significant differences between RA patients and healthy controls regarding age, gender or BMI (Table 1).

Increased concentrations and sizes of EVs in plasma of RA patients

RA patients showed a significantly ($p = 1.2^{*}10^{-12}$) higher concentration of plasma EVs than the healthy controls (Fig. 1a). The size of the EVs ranged from 50 to 350 nm in both cohorts with a significantly greater mean (148 nm vs. 129 nm; $p = 0.0001$) and mode (120 nm vs. 104 nm; $p = 0.0007$) size in RA patients (Fig. 1a). The size estimates were confirmed by transmission electron microscopy (TEM) (Fig. 1b). No correlations were seen between EV concentration or EV size and clinical variables, like CRP, ESR and DAS28, within the RA cohort (Supplementary Table 1). The presence of EV markers CD63, CD9 and TSG101 was confirmed by Western blot (Fig. 1c, Supplementary Fig. 1). We also detected albumin in the EV preparations, but this was expected as high levels of albumin are present in blood plasma, both as soluble protein and bound to the EVs as part of the EV protein corona[9,14], and size exclusion chromatography (SEC) is known to co-isolate some non-EV particles. Taken together, the RA patients had more and larger EVs in their plasma compared to controls.

The identified proteins showed EV origin

Proteomic analysis reliably quantified 682 proteins in our EV preparations ($N = 49$) from both RA patients and controls (Supplementary Dataset File 1). Most of these proteins (97%) had previously been detected in EVs, as reported by Vesiclepedia, (Supplementary Fig. 2a) with 72 proteins among the top 100 (Supplementary Fig. 2b; Supplementary Dataset File 2). This included the EV associated markers PDCD6IP, GAPDH, HSPA8, ACTB, ANXA2 and CD9. Gene ontology analysis of cellular component confirmed that proteins originated from extracellular exosomes (an EV subtype), the plasma membrane and microvesicles (Supplementary Fig. 2c). We also found an involvement of the immune system as expected in blood plasma EVs. Among the most prominent pathways were signal transduction, post-translational protein modification and neutrophil degranulation (Supplementary Fig. 2c).

Most of the 682 proteins (86%) were found in both cohorts, while 62 and 31 proteins were only reliably quantified in patients and controls, respectively (Supplementary Fig. 3, Supplementary Dataset File 3). However,

	RA ($n = 32$)	HC ($n = 20$)	p-value
Female [in %]	32 [100]	20 [100]	1
Age (median[range])	48 [18–71]	40 [19–59]	0.1
BMI (median[range])	25 [20–36]	25 [21–36]	0.8
ACPA positive [in%]	32 [100]	NA	NA
RF positive [in %]	24 [75]	NA	NA
CRP (median [range])	5 [0-108]	NA	NA
ESR (median[range])	21 [5–81]	NA	NA
TJC (median[range])	6 [1–26]	NA	NA
SJC (median[range])	5 [0–25]	NA	NA
DAS28 (median[range])	4.7 [2.9–8.3]	NA	NA
Never smoked [in %]	19 [59]	NA	NA
Former smoker [in %]	9 [28]	NA	NA
Active smoker [in %]	4 [13]	NA	NA

Table 1. Demographic and clinical characteristics of the treatment naïve RA patients at baseline and healthy controls. RA: Rheumatoid arthritis; HC: Healthy control; BMI: Body mass index; ACPA: Anti-citrullinated protein antibodies; RF: Rheumatoid factor; CRP: C-reactive protein; ESR: Erythrocyte sedimentation rate; TJC: Tender joint count; SJC: Swollen joint count; DAS28: Disease activity score 28; NA: Not applicable.

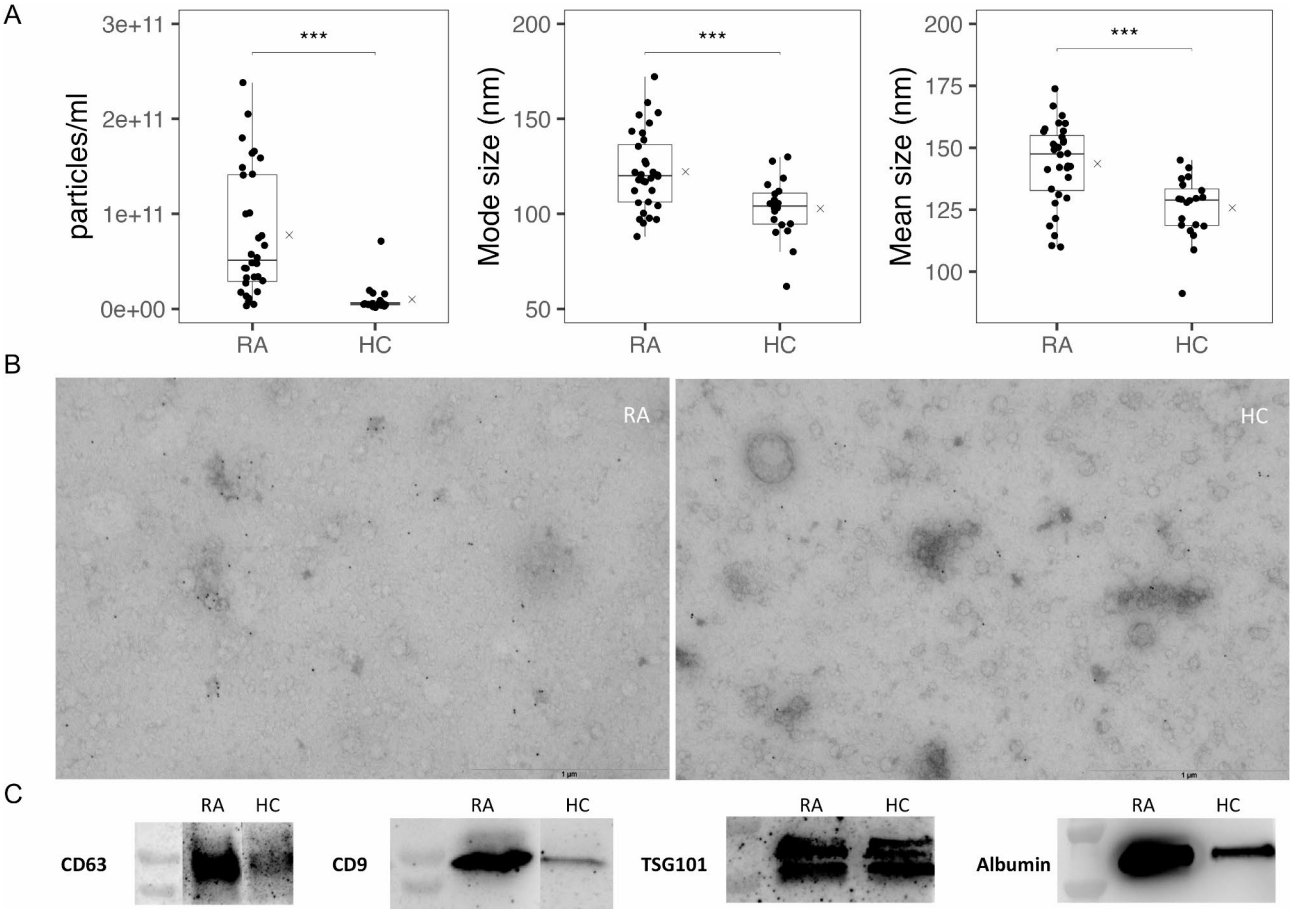

Fig. 1. Quantitation and characterization of EVs in RA patients and healthy controls by (a) measuring particle concentration, mode and mean size (x represents group mean), with mode size referring to the most frequently occurring particle size, (b) transmission electron microscopy micrographs with anti-CD63 immunostaining and (c) western blotting of EV generic markers CD63, CD9 and TSG101 and the non-EV marker albumin. RA: Rheumatoid arthritis; HC: healthy controls.

these cohort exclusive proteins were identified only in few samples and variable samples and were discarded due to lack of statistical power.

Quantitative differences in EV protein levels between RA patients and controls

Next, proteins reliably quantified in at least 50% of patients or controls ($N = 430$) were included in the quantitative comparison analysis of protein levels (Supplementary Dataset File 4). Principal component analysis of the quantitative proteomic data showed distinct clustering of the healthy controls and RA patients (Fig. 2a). Furthermore, we detected significant differential protein levels between RA patients and controls (Supplementary Fig. 4). Higher levels were observed in RA patients for 26 proteins (Supplementary Fig. 5, Supplementary Table 2), and the most significant (P_{adj}<0.0001) were the acute phase proteins SAA1 and S100A9 (Fig. 2b). Reduced protein levels in RA patients were seen for 31 proteins (Supplementary Fig. 6, Supplementary Table 3), with PRDX2, OIT3, FN1, APOC2, APOC3 and VWF being most significant ($P_{adj} < 0.0001$; Fig. 2b).

We next used the Human Protein Atlas[15](proteinatlas.org) to explore the RNA expression of the differentially expressed EV proteins, to indicate their possible tissues and cells of origin (Fig. 3, Supplementary Tables 2 and 3). Interestingly, 16 of these 57 proteins were mainly expressed in liver and hepatocytes, where many plasma proteins are produced. Most (21/26) of the EV proteins increased in RA were expressed in immune cells, either broadly across all cell types or by granulocytes (mostly neutrophils), while only half (16/31) of the EV proteins reduced in RA were expressed in immune cells.

Pathway analysis showed that 15 of the differentially expressed proteins interact in a network comprising inflammatory disease and inflammatory response (Fig. 4a, Supplementary Table 4), where a central role was seen for activation of SAA (SAA1 and SAA2) and proteins of the tubulin family (TUBA1A, TUBB1 and TUBB4B), and inhibition of Peroxiredoxin-2 and lipoproteins (APOC2, APOC3 and APOC4). Four additional networks were identified, which also involved RA relevant functions like humoral response and inflammatory response.

Our 57 disease associated EV proteins were predicted to be regulated by eight common upstream regulators (Fig. 4b, Supplementary Table 5), several involved in immunological processes. In particular, the upstream regulators included the proinflammatory IL1, RELA involved in heterodimer formation of the transcription

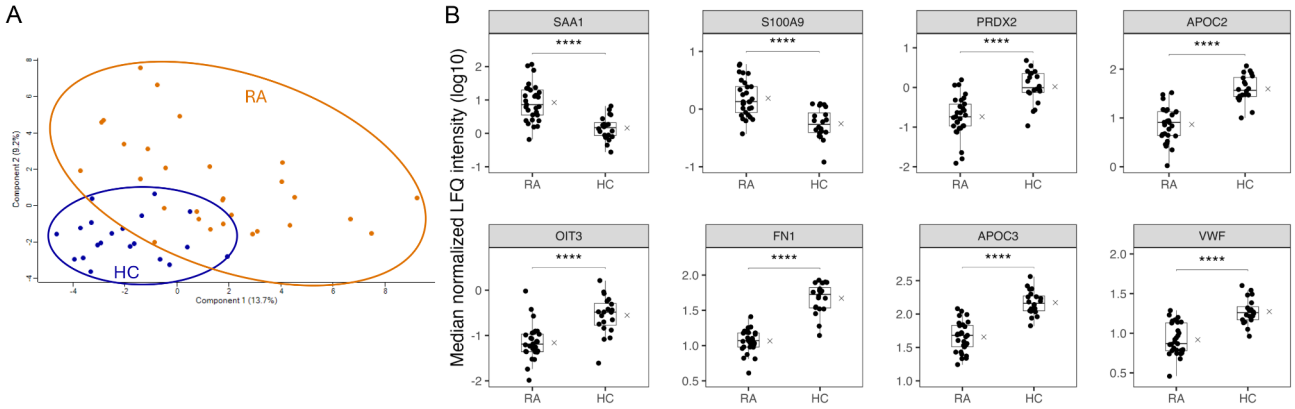

Fig. 2. Quantitative EV protein differences between RA patients and controls. (a) Principal component analysis of EV proteomes from RA patients and healthy controls, (b) detected levels of the most significantly RA associated EV proteins in cases and controls (x represents group mean). RA: Rheumatoid arthritis; HC: Healthy controls; **** = Padj < 0.0001.

log10 fold-change	p adj
0.95	0.001
0.87	0.001
0.76	<0.0001
0.69	0.02
0.6	0.009
0.56	0.004
0.54	0.03
0.53	0.021
0.51	0.024
0.5	0.009
0.48	0.028
0.47	0.002
0.47	0.012
0.47	0.035
0.45	0.043
0.45	0.02
0.44	<0.0001
0.43	0.006
0.4	0.02
0.4	0.036
0.38	0.005
0.36	0.027
0.34	0.021
0.32	0.033
0.31	0.004
0.31	0.02
-0.3	0.04
-0.3	0.004
-0.3	0.01
-0.31	0.004
-0.32	0.008
-0.33	0.004
-0.33	0.05
-0.33	0.009
-0.34	0.03
-0.35	<0.0001
-0.36	0.002
-0.37	0.02
-0.38	0.007
-0.39	0.03
-0.4	0.03
-0.43	0.004
-0.44	0.004
-0.44	0.01
-0.45	0.002
-0.48	0.01
-0.5	0.02
-0.51	<0.0001
-0.53	0.02
-0.57	0.004
-0.57	0.002
-0.6	<0.0001
-0.6	0.009
-0.61	<0.0001
-0.66	0.004
-0.73	<0.0001
-0.76	<0.0001

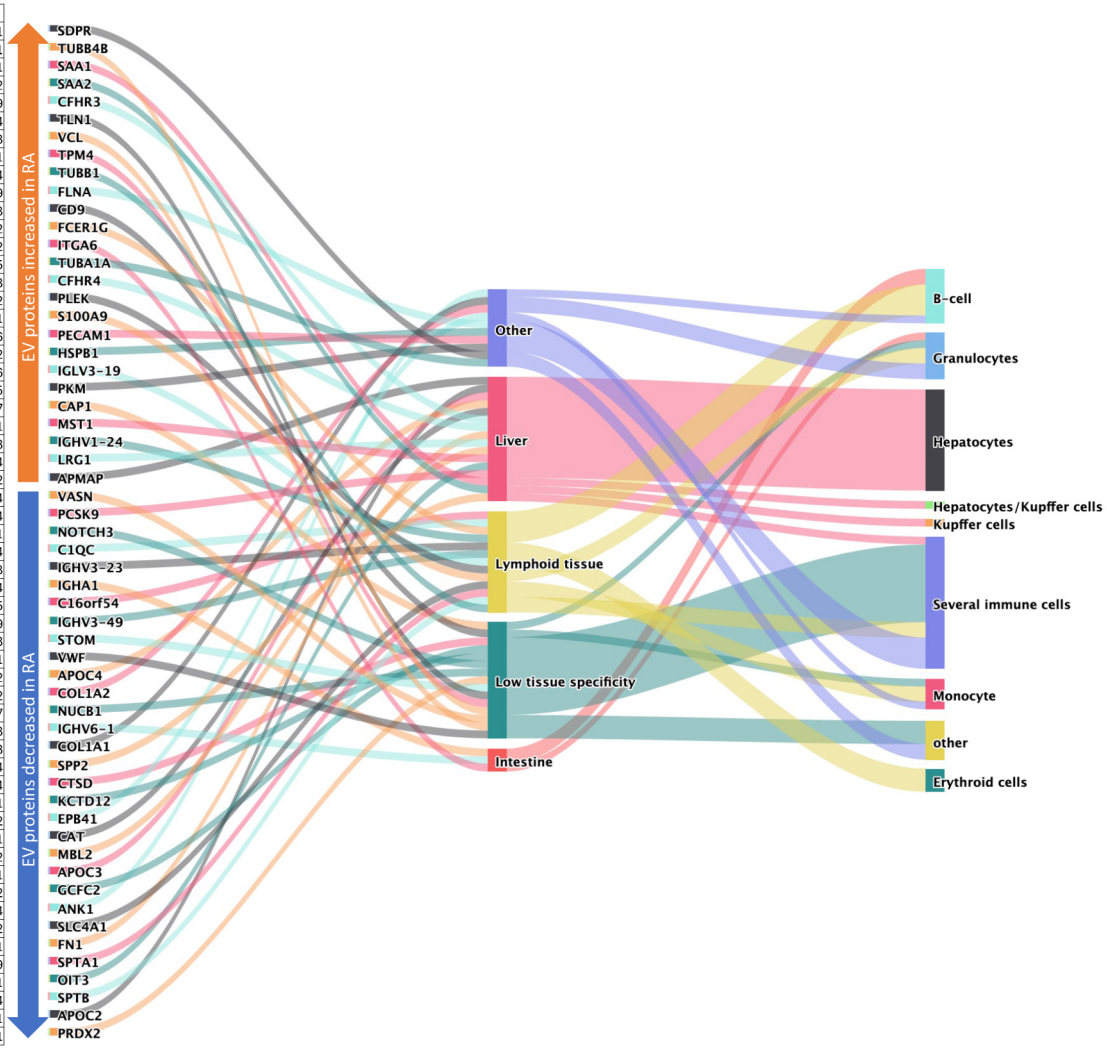

Fig. 3. Potential cell and tissue origin of RA associated EV proteins. The plot highlights our main findings as reported by gene expression across cell and tissue types in the Human Protein Atlas and the proteins' corresponding fold-change and adjusted p-values detected in our DE analysis.

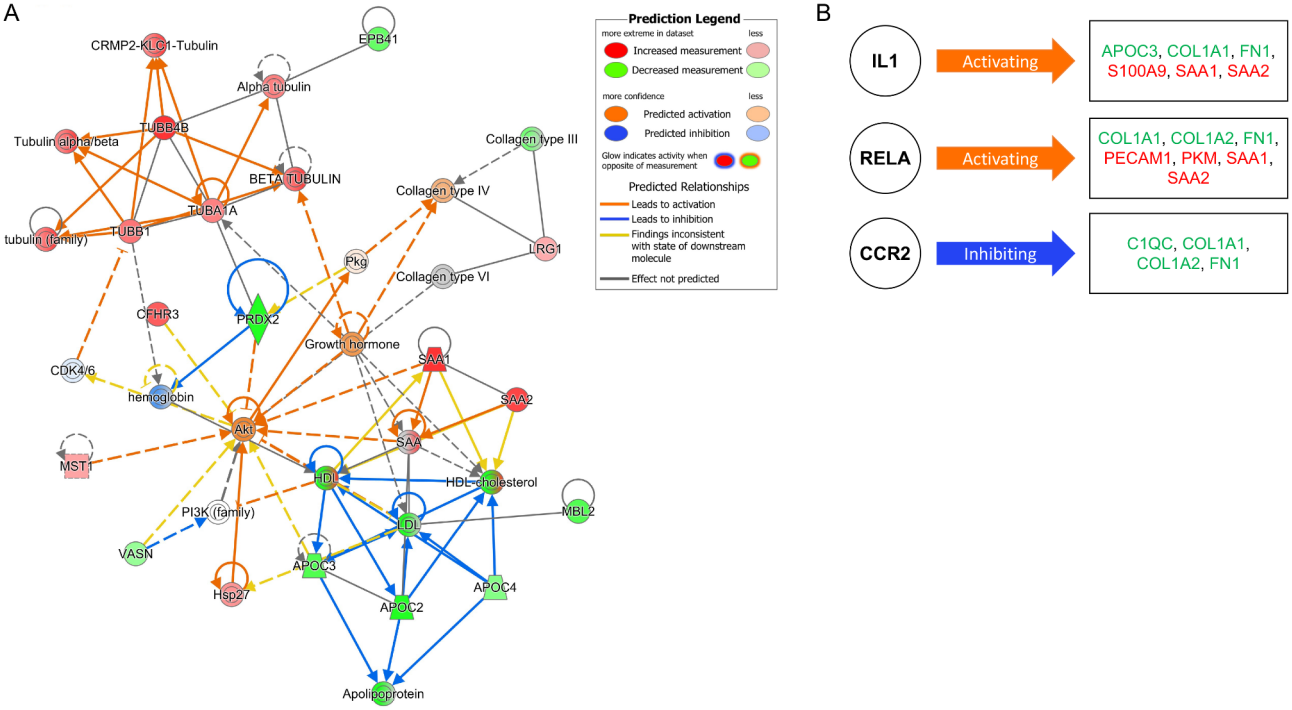

Fig. 4. Predicted biological networks and upstream regulators for the RA associated EV proteins. (a) the top network related to inflammatory disease, inflammatory response, organismal injury and abnormalities, (b) the three most RA relevant upstream regulators. Analysis was done using Ingenuity pathway analysis.

factor NF-κB, and CCR2 believed to be involved in cell recruitment to the synovial compartment. Interestingly, the upregulated SAA1 and SAA2 acute phase reactants were targets for all activated upstream regulators.

Protein cargo of EVs correlated with RA disease activity

We next addressed whether the RA associated EV proteins were also associated with disease activity, and 10 proteins significantly correlated with DAS28 (Supplementary Dataset File 5). Three of these showed a positive correlation with DAS28 (SAA1, LRG1 and IGLV3-19), and were also increased in RA patients compared to controls. The seven remaining EV proteins were negatively correlated with DAS28, and some were decreased in RA (SLC4A1, C1Q, SPP2, and SPTA1), while others (SDPR, TLN1 and APMAP) were increased in RA compared to HC.

SAA1 levels in EVs were hence associated with both RA development and disease activity. The SAA1 and SAA2 are isoforms of the RA inflammatory marker SAA (25), and their EV protein levels correlated ($r = 0.77$, $P = 2.8E\text{-}05$, Supplementary Fig. 7b). Furthermore, EV SAA1 and SAA2 were also positively correlated with CRP and ESR (Supplementary Fig. 7a, Supplementary Table 6). We next attempted to relate these EV findings to serum levels. High levels of serum SAA were detected in 61% of patients, and these levels, as well as those of the individual SAA1 and SAA2 isoforms were all positively correlated with CRP, ESR and DAS28 (Supplementary Fig. 7a, Supplementary Table 6). Finally, serum total SAA levels reflected EV SAA1 ($r = 0.91$) and EV SAA2 ($r = 0.77$) levels (Supplementary Fig. 7c).

Several RA associated EV cargo proteins were not detected among total serum proteins

To shed light on the importance of EV protein transport in the RA pathogenesis, we compared proteomic data from total serum (Supplementary Dataset File 6) to plasma EV proteins. Fewer proteins were reliably quantified from total serum ($N = 343$, Supplementary Dataset File 7) compared to the plasma EVs, and less than half of the EV associated proteins were reliably quantified in the serum samples (Fig. 5, Supplementary Dataset File 8). Specifically, only 42% of the RA associated EV proteins ($N = 57$) were reliably quantified in serum. As few as, ten proteins (SAA1, SAA2, CFHR4, APOC3, VWF, APOC4, C1QC, IGHA1, MBL2, IGHV6-1) had levels that significantly correlated ($0.4 < r < 0.8$) between total serum and plasma EVs, with SAA1 showing the strongest correlation (Supplementary Table 7). Furthermore, there was an overrepresentation of liver restricted production of the EV proteins found to correlate with serum (6/10). Overall, most RA associated EV derived proteins (58%) could either not be detected, or lack RA association, in total serum.

Discussion

In this study, we revealed that our newly diagnosed, DMARD naïve RA patients had higher concentrations and larger EVs than healthy controls. Furthermore, the RA patients had a distinct EV protein profile with 57 associated proteins implicated in inflammatory networks and with RA relevant upstream regulators. Some of

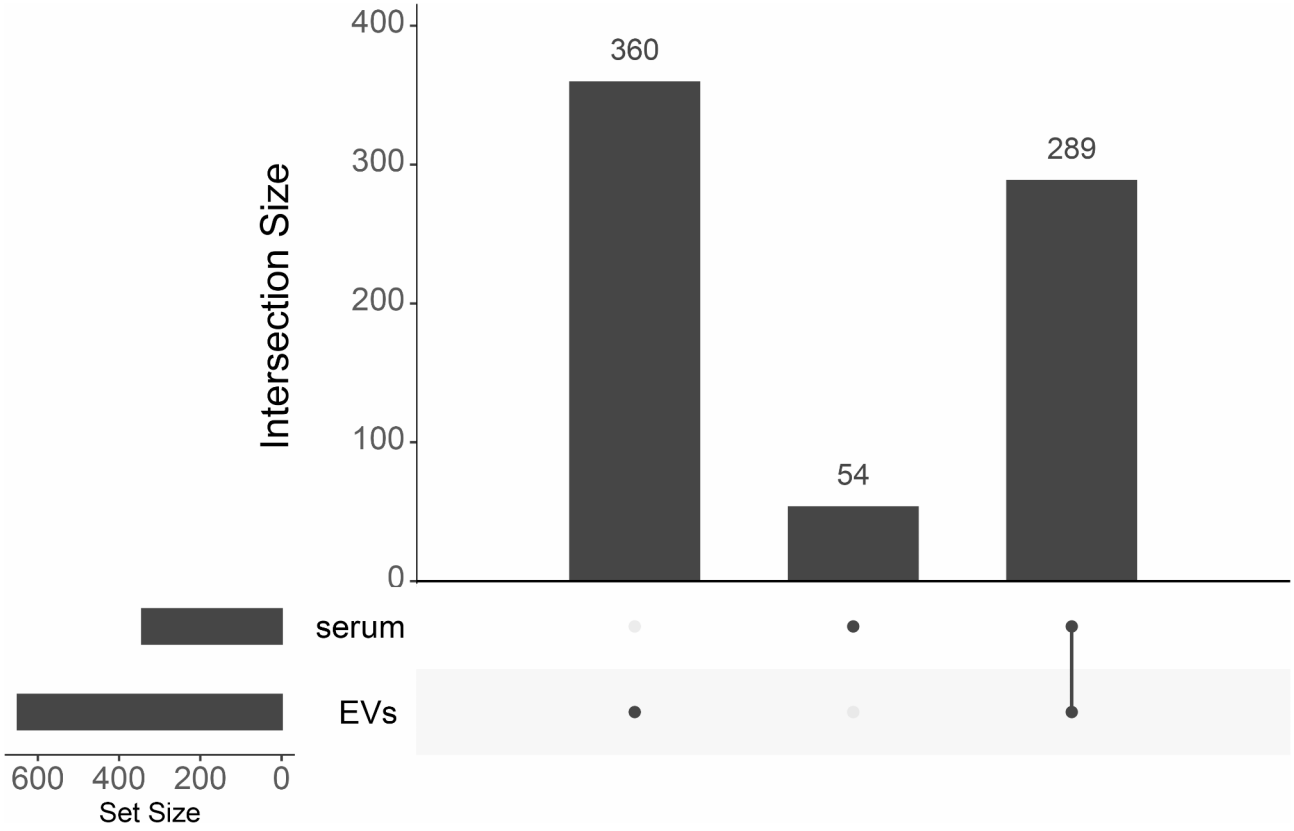

Fig. 5. Number of proteins reliably quantified in plasma EVs, total serum, or both. The analysis highlights shared and unique protein profiles between EVs and serum samples in the 28 RA patients.

the EV proteins were also associated with disease activity. Only few RA associated EV proteins correlated with serum levels of the same protein. Taken together, our data indicate an important immunological role of EVs in cell-cell communication during the pathogenesis of RA and emphasize the importance of investigating proteins also on an EV level.

In line with our findings, increased amounts of EVs in plasma from RA patients have previously been reported[12,16–19], except in one publication[20]. Some of these studies also showed a positive correlation between EV concentration and either disease activity[16,17] or RA inflammatory markers[19]. However, we did not detect any association between EV amounts and disease activity in our RA cohort. There are several factors that distinguish our study from the aforementioned studies which may have affected the EV populations. In contrast to our newly diagnosed, treatment naive patients, all studies but one[16–20] included patients with established disease (mean disease duration 4.9–13 years) who underwent various drug treatment regimes. The study cohorts also differed in DAS28, gender ratios, age at inclusion and smoking status[21–23]. Furthermore the statistical power differed between the RA cohorts, (19[16] to 114[18] patients), and a variety of EV enrichment methods were used, all with a tradeoff between yield and purity[24]. Taken together, EV release is most likely increased in RA, while more studies are needed to settle the role of EV concentrations in relation to clinical aspects of RA.

To date, EV isolations suffer from contamination, however, we have confirmed the presence of EVs visually and the vast majority of the reliably quantified proteins are of EV origin, as reported by Vesiclepedia[25]. Furthermore, we observed the presence of known EV surface markers for exosomes (CD63, CD9 and TSG101), which in a semiquantitative way also confirmed a higher EV amount in RA patients versus controls. Together our results show that our samples are clearly EV enriched, although the exact ratio of EVs and contaminants is unknown.

Our results demonstrated a distinct difference in EV protein profiles between treatment naïve RA patients and healthy controls, with both higher and lower levels of specific EV proteins in RA patients. These proteins were RA relevant, taking part in inflammatory and immunological pathways. In addition, the generic EV marker CD9 was clearly upregulated in RA compared to healthy controls, which corresponds to our previous findings measuring tetraspanins on single EVs[26]. CD9 associate with ADAM10, among other proteins, which influence antibody production and inflammatory response[27]. The role of EVs in autoimmune diseases have been suggested to involve release of EVs containing autoantigens or proinflammatory cytokines, as well as EVs interacting with antibodies in the formation of immune complexes[8]. Interestingly, six of our RA associated EV proteins were immunoglobulins. We also observed several inflammatory proteins, including SAA1, SAA2 and S100A9, increased in EVs from RA patients. Furthermore, our RA associated EV proteins were shown by pathway analysis to have three upstream activators, RELA, LPS and IL1, which are regulators of SAA1, SAA2 and S1009A, but not themselves detected in our EV preparations. Hence, our study suggests an involvement of

immunomodulatory EVs in RA, and the RA associated EV proteins warrants confirmation in larger replication cohorts of newly diagnosed, DMARD naïve patients.

The heterodimers S100A8 and S100A9, forming calprotectin, were detected in our EV dataset, however, only S100A9 was observed at a significantly increased level in RA patients. These alarmins are expressed by neutrophils and have been reported to be key plasma biomarkers in RA[28]. In contrast to our findings, Seny et al. found S100A9 in serum to positively correlate with CRP and DAS28 in RA patients[29], while we did not detect S100A9 in our total serum proteomics analysis, which is in line with other studies and could be explained by the resistance of serum calprotectin to digestion hampering the mass spectrometry analysis[28]. Interestingly, neutrophils release several types of EVs[30] including elongated neutrophil-derived structures (ENDS), which are enriched in S100A8 and S100A9 [31]. Upon inflammatory signals, neutrophils roll on the endothelium before they arrest to enter the inflamed tissue. The rolling is stabilized by formation of tethers, which can break, and form ENDS that detach and become spherical vesicles of approximately 115 nm[31]. Our EV protein profile had neutrophil degranulation as one of the top pathways, in line with what is seen for ENDS proteins. Hence, further investigations are needed to reveal the functional role of S100A9 in RA, and in particular, whether the RA association involves release by ENDS or other neutrophilic vesicles.

Interestingly, we detected a significant correlation between RA disease activity measurements and EV derived SAA1 or SAA2 levels. We related our EV findings to the serum levels of total SAA, SAA1 and SAA2 and observed that all SAA measurements correlated positively with disease activity and each other. Accordingly, several studies have reported increased levels of SAA1 and total SAA in both serum, synovial fluid and EVs from RA patients, thereby proposing SAA as a marker of disease activity being even more sensitive than CRP or ESR (25). Functionally, SAAs promote proinflammatory cytokines and a pathogenic differentiation of T_H17 cells, but also have important roles in lipid transportation. SAA self-assembles with phospholipids to form stable protein-rich nanoparticles (from 10 to 100 nm) and has been hypothesized to function as a molecular mop clearing membrane debris from dead cells during inflammation[32]. Hence, further studies into the role of free vs. lipid-bound SAA in RA pathogenesis are needed, particularly since it is also associated with increased risk of both cardiovascular disease and secondary amyloidosis in RA patients[33].

The fact that most RA associated EV derived proteins were not reflected in total serum stressed the importance of also assessing blood proteins on an EV level, as sample material influences and limits proteomic data methodologically. Furthermore, the discordance between serum and EV protein profiles and RA associations underpins the importance of EVs in cell-cell communication in RA.

Our study suggests that cell-cell communication via EVs is markedly upregulated in active RA, with alterations in EV protein cargo predicted to be involved in inflammatory processes with the activating upstream regulators RELA, LPS and IL1. The RA associated EVs appear to originate from mainly hepatocytes or immune cells, and interestingly the strongest RA associated EV proteins were inflammatory molecules, like SAA1 and S100A9, already suggested to be important biomarkers in RA. Interestingly, the protein levels detected in the EVs did generally not correlate with total serum protein levels, stressing the importance of further investigating the role of EVs and their cargo in RA.

Methods

We have submitted information from our experiments to the EV-TRACK knowledgebase (EV-TRACK ID: EV230998)[34].

Study population

This study included 32 RA patients diagnosed according to the 2010 RA classification criteria[6] recruited through the Norwegian Very Early Arthritis Clinic (NOR-VEAC) observational study (ISRCTN05526276). Patients were clinically assessed, and samples were collected at Diakonhjemmet Hospital ($N=13$), Lillehammer Hospital ($N=4$), Martina Hansen's Hospital ($N=5$), Betanien Hospital ($N=4$), Vestre Viken Hospital Trust ($N=2$) and Hospital of Southern Norway Trust ($N=4$). Patients with the following reasons for joint swelling was excluded: osteoarthritis, trauma, mechanical joint lesion (e.g. meniscus lesion), gout, pseudogout, septic arthritis and acute sarcoid arthropathy. The cohort included females aged 18–71 with arthritis less than 12 months duration. Onset of arthritis was defined as the time when at least one joint became swollen. Mean symptom duration was approximately 4 months. Blood plasma was collected at the time of inclusion when patients were newly diagnosed and DMARD naïve. Clinical parameters including ACPA, RF, C-reactive protein (CRP), erythrocyte sedimentation rate (ESR), 28-joint disease activity score (DAS28), smoking-status, age, gender and BMI were recorded upon inclusion. The following formula was used to calculate DAS28: $\text{DAS28-ESR}=(0.56 \times \sqrt{\text{TJC}}) + (0.28 \times \sqrt{\text{SJC}}) + (0.014 \times \text{PGA [mm]}) + (0.7 \times \ln [\text{ESR}])$.

Age, gender and BMI matched healthy controls ($N=20$, HC) were recruited among blood donors, through the CFS/ME center at Oslo University Hospital, thereby excluding presence of a large panel of diseases including rheumatic and coronary artery diseases.

The study was approved by the Regional Ethics committee of South East Norway (REK) and conducted in compliance with the Declaration of Helsinki. Written informed consent was obtained from all participants.

Sample preparation

Peripheral blood was collected in EDTA tubes. Patient tubes were centrifuged within 45 min at 1,600-2,500 g for 10–15 min at room temperature (RT), depending on the hospital's biobanking protocol, while control tubes were centrifuged within 30 min at 1,800 g for 15 min at RT. Control plasma subsequently underwent a 15,000 g centrifugation step for 15 min at 4 °C before storing the plasma at – 80 °C. Patient samples were also stored at – 80 °C, but some samples were first stored one day at – 20 °C. Plasma from RA samples were centrifuged at 15,000 g for 15 min at 4 °C after thawing to ensure similar conditions as the healthy controls.

Serum samples from 28 of the RA patients were collected in serum collection tubes either with ($n = 13$) or without gel ($n = 15$). Within 75 min, the samples were centrifuged at 1,600-2,200 g for 10–12 min at RT, depending on the biobanking protocol of the specific hospitals, and stored similarly as the plasma samples.

Plasma EV enrichment

All plasma samples were thawed at 4 °C. EVs were enriched utilizing size exclusion chromatography (SEC) by applying 500 µl plasma to the qEV original 70 nm column (Izon Science, Oxford, UK). SEC fraction 7–9 revealed the highest amounts of EVs and lowest amounts of contamination and were pooled. Freshly isolated material was used for nanoparticle tracking analysis (NTA), transmission electron microscopy (TEM) and protein isolation prior to western blotting (WB) while aliquots for liquid chromatography-tandem mass spectrometry (LC-MS/MS) were stored at – 80 °C prior to analysis.

Nanoparticle tracking analysis

SEC isolated EV preparations were diluted 1:100 in 0.02 µm freshly filtered PBS to a concentration recommended for NTA analysis on the Nanosight NS500 (Malvern Instruments Ltd, Malvern, UK). Samples were injected into the instrument at an infusion rate of 20 and measured as 60 s videos in triplicates. Size and concentration were calculated using NTA Software 3.4, build 3.4003 (Malvern). The analysis settings were adjusted to camera level 14/15 and detection threshold 4. Polystyrene beads (100 nm) were analyzed daily prior to and after measurements to ensure the stability of the analysis.

Transmission electron microscopy

For immuno-transmission electron microscopy (immuno-TEM), EVs were dropped directly onto formvar/carbon coated grids and left for 10 min at room temperature. Then EVs were fixed in 4% formaldehyde and 0.1% glutaraldehyde for 15 min. Grids were washed with PBS, blocked for 10 min with 0.5% bovine serum albumin in PBS, incubated for 20 min with mouse anti-CD63 primary antibody (M-a-CD63, Developmental Studies Hybridoma Bank, Iowa, USA), incubated 20 min with rabbit anti-mouse secondary antibody and, finally, incubated with protein A-gold (10 nm) for 15 min. Between each antibody incubation, grids were washed twice with PBS. Grids were then washed five times in PBS and five times in water and stained with 0.4% uranyl acetate and embedded in 1.8% methyl cellulose for 10 min at 4 °C. Grids were allowed to dry for 20 min and samples were observed on a JEOL-JEM 1230 at 80 kV and images were recorded with a Morada digital camera.

Western blotting

SEC enriched EV preparations from healthy controls and RA patients were pooled separately for western blotting. An additional concentration step of the pools, using the 3000 MWCO Amicon Ultra-2 ml centrifugal filter units (Merck, Darmstadt, Germany), was performed prior to CD63 western blotting analysis.

EVs from sample pools of the same volume were lysed by adding 10x RIPA (Merck Millipore) mixed with protease-phosphatase inhibitor (Thermo Fisher Scientific, Waltham, USA) and incubated on ice for 15 min. The EV proteins were stored at – 20 °C until analysis. Sample buffer was added to thawed EV proteins; 4x Laemmli sample buffer (Bio-Rad) for non-reducing conditions (CD63 and CD9) and 3x Sample buffer with DTT for reducing conditions (TSG101 and Albumin). Then, the samples were heated at 97 °C for 5 min. Proteins were separated on Mini-Protean®TGX™ 4–20% gels (Bio-Rad, California, USA) and transferred to 0.2 µm nitrocellulose membranes (Bio-Rad). Membranes were blocked with 5% BSA (CD63 and CD9) or 5% milk (TSG101 and Albumin) in tris-buffered saline (Bio-Rad) with 0.1% Tween 20 (Sigma-Aldrich, TBS-T) for 1 h at room temperature, before incubating with primary antibodies (CD63 monoclonal antibody (Ts63) 1:500, 10628D, Invitrogen; CD9 Monoclonal antibody (Ts9) 1:500, Invitrogen; TSG101 Monoclonal antibody (4A10) 1:1000, Invitrogen; ALB (F-10) 1:1000, Santa Cruz Biotechnology) overnight at 4 °C. The membranes were washed 3 times with TBS-T prior to 1 h incubation with horseradish peroxidase-linked secondary antibody (Anti-mouse IgG, Cell Signaling Technology) at room temperature. Three additional washing steps were then performed. Finally, the blots were incubated in ECL™ Prime Western Blotting Detection Reagents (Cytiva, Massachusetts, USA) and imaged with ImageQuant LAS4000 (Cytiva).

Label-free liquid chromatography mass spectrometry

EV and serum proteins were assessed by label-free quantitative proteomics at the Proteomics Core Facility, University of Oslo and Oslo University Hospital.

EV samples: EVs were lysed by adding 1% ProteaseMax Surfactant (Promega, Madison Wisconsin, United States) in 50 mM NH_4HCO_3 followed by vortexing and heating at 95 °C for 20 min. Protein concentrations were measured by BCA assays. The proteins were reduced by addition of 0.5 M DTT to a final concentration of 10 mM and incubation at 56 °C for 30 min. Then, to alkylate proteins, 3.2 µl of 550 mM IAA was added to a final concentration of 15 mM and samples were incubated at RT in the dark for one hour. Samples were diluted with 50 mM NH_4HCO_3 to a final ProteaseMax concentration of 0.033% and trypsin (Promega) was added to the samples followed by overnight incubation at 37 °C. The resulting peptides were concentrated and desalted before mass spectrometry (MS) analysis using the STAGE-TIP method with C18 resin disk (Affinisep, Normandy, France).

Serum samples: 5 µl of serum was precipitated with 70% acetonitrile onto magnetic beads (MagReSynAmine, Resyn Biosciences). The proteins were washed on the beads with 100% acetonitrile, 70% ethanol and then resuspended in 100 µl 50 mM NH_4HCO_3. The proteins were reduced and alkylated in the same manner as the EV proteins before 0.5 µg trypsin was added for overnight on-beads protein digestion at 37 °C. The resulting peptides were further processed as the EV samples.

LC-MS/MS analysis of both EV and serum samples was done on a nanoElute UHPLC coupled to a timsTOFfleX mass spectrometer (Bruker Daltonics, Bremen, Germany) via a CaptiveSpray ionsource. Peptides were separated on a 25 cm reversed-phase C18 column (1.6 µm bead size, 120 Å pore size, 75 µm inner diameter, Ion Optics) with a flow rate of 0.3 µl/min and a solvent gradient from 0 to 35% B in 60 min. Solvent B was 100% acetonitrile in 0.1% formic acid and solvent A 0.1% formic acid in water. The mass spectrometer was operated in data-dependent Parallel Accumulation-Serial Fragmentation (PASEF) mode. Mass spectra for MS and MS/MS scans were recorded between m/z 100 and 1700. Ion mobility resolution was set to 0.60–1.60 V·s/cm over a ramp time of 100 ms. Data-dependent acquisition was performed using 10 PASEF MS/MS scans per cycle with a near 100% duty cycle. A polygon filter was applied in the m/z and ion mobility space to exclude low m/z, singly charged ions from PASEF precursor selection. An active exclusion time of 0.4 min was applied to precursors that reached 20 000 intensity units. Collisional energy was ramped stepwise as a function of ion mobility.

Proteomic data analysis

Protein identification and label-free quantification was done using MaxQuant version 2.0.1.0.

Carbamidomethyl was set as a fixed modification and acetyl carbamyl and oxidation were set as variable modifications. First search peptide tolerance of 20 ppm and main search error 4.5 ppm were used. Trypsin without proline restriction enzyme option was used, with two allowed miscleavages. The minimal unique + razor peptides number was set to 1, and the allowed false discovery rate (FDR) was 0.01 (1%) for peptide and protein identification. Label-free quantitation (LFQ) was employed with default settings. UniProt database with 'Human' entries (2022) was used for the database searches. The mass spectrometry EV proteomics data have been deposited to the ProteomeXchange Consortium via the PRIDE[35] partner repository with the dataset identifier PXD060460.

Further data analysis was performed using LFQ intensity measurements which includes normalization and reduction of bias to improve accuracy. Data filtering and statistical analysis was done using Perseus software version 2.0.7.0 [36] with LFQ intensities as input, excluding contaminants and proteins identified by site. In Perseus, LFQ values were log10 transformed, and data was filtered with a minimum of 50% valid values in at least one group followed by standard imputation from normal distribution. Based on principal component analysis three samples were considered as outliers and omitted from further analysis. The data was median normalized and MS batch corrected by Combat using PerseusR[37] before statistical analysis. Venn diagrams of the EV proteins were generated using FunRich functional enrichment analysis tool version 3.1.3 [38]. DAVID functional annotation tool[39,40] was utilized for gene ontology analysis. For pathway analysis, the results from statistical analysis done in Perseus were uploaded into Ingenuity® Pathway Analysis (IPA, Qiagen)[41]. The analysis settings in IPA were set to a cut-off at p-value = 0.05, FDR = 0.05 and a minimum of a two-fold change difference in EV protein expression between RA patients and healthy controls.

Serum SAA

Serum Amyloid A (SAA) in total serum was measured (reportable interval 3-200 mg/L) in 28 RA samples with latex-enhanced immunonephelometry on BNII from Siemens Healthcare AS at the Department of Medical Biochemistry, Oslo University Hospital. SAA levels > 6.4 mg/l were regarded as high as according to manufacturer (Siemens Healthcare, Erlangen, Germany). Calibrator traceability was in accordance with the 1st International WHO Standard 92/680. Patient samples showed excellent repeatability when measured in duplicates with a CV < 7%.

Statistical analyses

Normality distribution and equality of variances in the data were assessed by Shapiro-Wilk test and Levene's test, respectively. Skewed data with unequal variances were submitted to Brunner-Munzel test while the non-parametric Mann-Whitney U test was used for skewed data with equal variances. Normally distributed data with equal variances were analyzed by Student's *t*-test. A p-value < 0.05 was deemed statistically significant. Correlation analysis was performed calculating the Pearson Correlation Coefficient (r), where some variables (CRP, ESR, BMI, EV SAA1/2, serum total SAA, serum SAA1/2) were log10 transformed to fulfil the normality assumption. The aforementioned statistical analyses of demographic variables and nanoparticle tracking analysis data were performed using R version 4.2.2.

We utilized the Perseus software v2.0.7.0 for proteomic differential expression analysis by two-sample *t*-test with permutation-based FDR ≤ 0.05 and p_{adj}-value cut-off < 0.05. Proteins ≥ 2-fold (2-fold change: log10-fold change = 0.3) differentially expressed between the groups were considered biologically significant.

Data availability

All data generated and/or analyzed during this study are included in this published article and its supplementary information files, and the mass spectrometry EV proteomics data have been deposited to the ProteomeXchange Consortium via the PRIDE partner repository (https://www.ebi.ac.uk/pride/) with the dataset identifier PXD060460.

Received: 16 December 2024; Accepted: 27 March 2025
Published online: 04 April 2025

References

1. Smolen, J. S., Aletaha, D. & McInnes, I. B. Rheumatoid arthritis. *Lancet* **388**, 2023–2038. https://doi.org/10.1016/S0140-6736(16)30173-8 (2016).

2. Vicente, G. N. S. et al. Cardiovascular risk comorbidities in rheumatoid arthritis patients and the use of anti-rheumatic drugs: a cross-sectional real-life study. *Adv. Rheumatol.* **61**, 38. https://doi.org/10.1186/s42358-021-00186-4 (2021).
3. Couderc, M. et al. Prevalence of renal impairment in patients with rheumatoid arthritis: results from a Cross-Sectional multicenter study. *Arthritis Care Res. (Hoboken)*. **68**, 638–644. https://doi.org/10.1002/acr.22713 (2016).
4. Smolen, J. S. et al. Rheumatoid arthritis. *Nat. Rev. Dis. Primers* **4**, 18001. https://doi.org/10.1038/nrdp.2018.1 (2018).
5. Schioppo, T., Ubiali, T., Ingegnoli, F., Bollati, V. & Caporali, R. The role of extracellular vesicles in rheumatoid arthritis: a systematic review. *Clin. Rheumatol.* **40**, 3481–3497. https://doi.org/10.1007/s10067-021-05614-w (2021).
6. Aletaha, D. et al. Rheumatoid arthritis classification criteria: an American College of Rheumatology/European League Against Rheumatism collaborative initiative. *Arthritis Rheum.* **62**, 2569–2581. https://doi.org/10.1002/art.27584 (2010).
7. van Boekel, M. A., Vossenaar, E. R., van den Hoogen, F. H. & van Venrooij, W. J. Autoantibody systems in rheumatoid arthritis: specificity, sensitivity and diagnostic value. *Arthritis Res.* **4**, 87–93. https://doi.org/10.1186/ar395 (2002).
8. Lu, M. et al. The role of extracellular vesicles in the pathogenesis and treatment of autoimmune disorders. *Front. Immunol.* **12**, 566299. https://doi.org/10.3389/fimmu.2021.566299 (2021).
9. Toth, E. A. et al. Formation of a protein Corona on the surface of extracellular vesicles in blood plasma. *J. Extracell. Vesicles* **10**, e12140. https://doi.org/10.1002/jev2.12140 (2021).
10. Burbano, C. et al. Extracellular vesicles are associated with the systemic inflammation of patients with seropositive rheumatoid arthritis. *Sci. Rep.* **8**, 17917. https://doi.org/10.1038/s41598-018-36335-x (2018).
11. Foers, A. D. et al. Proteomic analysis of extracellular vesicles reveals an Immunogenic cargo in rheumatoid arthritis synovial fluid. *Clin. Transl. Immunol.* **9**, e1185. https://doi.org/10.1002/cti2.1185 (2020).
12. Ucci, F. M. et al. Citrullinated and carbamylated proteins in extracellular microvesicles from plasma of patients with rheumatoid arthritis. *Rheumatol. (Oxf.)* https://doi.org/10.1093/rheumatology/keac598 (2022).
13. Qin, Q. et al. Systemic proteomic analysis reveals distinct exosomal protein profiles in rheumatoid arthritis. *J. Immunol. Res.* **2021**, 9421720. https://doi.org/10.1155/2021/9421720 (2021).
14. Wolf, M. et al. A functional Corona around extracellular vesicles enhances angiogenesis, skin regeneration and Immunomodulation. *J. Extracell. Vesicles.* **11**, e12207. https://doi.org/10.1002/jev2.12207 (2022).
15. Sjostedt, E. et al. An atlas of the protein-coding genes in the human, pig, and mouse brain. *Science* **367**, 456. https://doi.org/10.1126/science.aay5947 (2020).
16. Knijff-Dutmer, E. A. J., Koerts, J., Nieuwland, R., Kalsbeek-Batenburg, E. M. & van de Laar, M. A. F. J. Elevated levels of platelet microparticles are associated with disease activity in rheumatoid arthritis. *Arthritis Rheum-Us* **46**, 1498–1503. https://doi.org/10.1002/art.10312 (2002).
17. Sellam, J. et al. Increased levels of Circulating microparticles in primary Sjogren's syndrome, systemic lupus erythematosus and rheumatoid arthritis and relation with disease activity. *Arthritis Res. Ther.* **11**, R156. https://doi.org/10.1186/ar2833 (2009).
18. Rodriguez-Carrio, J. et al. Altered profile of circulating microparticles in rheumatoid arthritis patients. *Clin. Sci. (Lond.)* **128**, 437–448. https://doi.org/10.1042/CS20140675 (2015).
19. Stojanovic, A. et al. Increased expression of extracellular vesicles is associated with the procoagulant state in patients with established rheumatoid arthritis. *Front. Immunol.* **12**, 718845. https://doi.org/10.3389/fimmu.2021.718845 (2021).
20. Arntz, O. J. et al. Rheumatoid arthritis patients with circulating extracellular vesicles positive for IgM rheumatoid factor have higher disease activity. *Front. Immunol.* **9**, 2388. https://doi.org/10.3389/fimmu.2018.02388 (2018).
21. Wu, F. et al. Smoking induced extracellular vesicles release and their distinct properties in Non-Small cell lung cancer. *J. Cancer* **10**, 3435–3443. https://doi.org/10.7150/jca.30425 (2019).
22. Baek, R., Varming, K. & Jorgensen, M. M. Does smoking, age or gender affect the protein phenotype of extracellular vesicles in plasma? *Transfus. Apher Sci.* **55**, 44–52. https://doi.org/10.1016/j.transci.2016.07.012 (2016).
23. Sun, B., Fernandes, N. & Pulliam, L. Profile of neuronal exosomes in HIV cognitive impairment exposes sex differences. *AIDS* **33**, 1683–1692. https://doi.org/10.1097/QAD.0000000000002272 (2019).
24. Thery, C. et al. Minimal information for studies of extracellular vesicles 2018 (MISEV2018): a position statement of the international society for extracellular vesicles and update of the MISEV2014 guidelines. *J. Extracell. Vesicles* **7**, 1535750. https://doi.org/10.1080/20013078.2018.1535750 (2018).
25. Pathan, M. et al. Vesiclepedia 2019: a compendium of RNA, proteins, lipids and metabolites in extracellular vesicles. *Nucleic Acids Res.* **47**, D516–D519. https://doi.org/10.1093/nar/gky1029 (2019).
26. Rydland, A., Heinicke, F., Flam, S. T., Mjaavatten, M. D. & Lie, B. A. Small extracellular vesicles have distinct CD81 and CD9 tetraspanin expression profiles in plasma from rheumatoid arthritis patients. *Clin. Exp. Med.* https://doi.org/10.1007/s10238-023-01024-1 (2023).
27. Smith, T. M. Jr., Tharakan, A. & Martin, R. K. Targeting ADAM10 in cancer and autoimmunity. *Front. Immunol.* **11**, 499. https://doi.org/10.3389/fimmu.2020.00499 (2020).
28. Nys, G. et al. Targeted proteomics reveals serum amyloid A variants and alarmins S100A8-S100A9 as key plasma biomarkers of rheumatoid arthritis. *Talanta* **204**, 507–517. https://doi.org/10.1016/j.talanta.2019.06.044 (2019).
29. de Seny, D. et al. Monomeric calgranulins measured by SELDI-TOF mass spectrometry and calprotectin measured by ELISA as biomarkers in arthritis. *Clin. Chem.* **54**, 1066–1075. https://doi.org/10.1373/clinchem.2007.099549 (2008).
30. Marki, A. & Ley, K. The expanding family of neutrophil-derived extracellular vesicles. *Immunol. Rev.* **312**, 52–60. https://doi.org/10.1111/imr.13103 (2022).
31. Marki, A. et al. Elongated neutrophil-derived structures are blood-borne microparticles formed by rolling neutrophils during sepsis. *J. Exp. Med.* **218** https://doi.org/10.1084/jem.20200551 (2021).
32. Frame, N. M., Jayaraman, S., Gantz, D. L. & Gursky, O. Serum amyloid A self-assembles with phospholipids to form stable protein-rich nanoparticles with a distinct structure: a hypothetical function of SAA as a molecular mop in immune response. *J. Struct. Biol.* **200**, 293–302. https://doi.org/10.1016/j.jsb.2017.06.007 (2017).
33. Soric Hosman, I., Kos, I. & Lamot, L. Serum amyloid A in inflammatory rheumatic diseases: a compendious review of a renowned biomarker. *Front. Immunol.* **11**, 631299. https://doi.org/10.3389/fimmu.2020.631299 (2020).
34. Consortium, E. T. et al. EV-TRACK: transparent reporting and centralizing knowledge in extracellular vesicle research. *Nat. Methods*. **14**, 228–232. https://doi.org/10.1038/nmeth.4185 (2017).
35. Perez-Riverol, Y. et al. The PRIDE database resources in 2022: a hub for mass spectrometry-based proteomics evidences. *Nucleic Acids Res.* **50**, D543–D552. https://doi.org/10.1093/nar/gkab1038 (2022).
36. Tyanova, S. et al. The perseus computational platform for comprehensive analysis of (prote)omics data. *Nat. Methods*. **13**, 731–740. https://doi.org/10.1038/nmeth.3901 (2016).
37. Rudolph, J. D. & Cox, J. A network module for the perseus software for computational proteomics facilitates proteome interaction graph analysis. *J. Proteome Res.* **18**, 2052–2064. https://doi.org/10.1021/acs.jproteome.8b00927 (2019).
38. Fonseka, P., Pathan, M., Chitti, S. V., Kang, T. & Mathivanan, S. FunRich enables enrichment analysis of omics datasets. *J. Mol. Biol.* **433**, 166747. https://doi.org/10.1016/j.jmb.2020.166747 (2021).
39. Huang da, W., Sherman, B. T. & Lempicki, R. A. Systematic and integrative analysis of large gene lists using DAVID bioinformatics resources. *Nat. Protoc.* **4**, 44–57. https://doi.org/10.1038/nprot.2008.211 (2009).
40. Sherman, B. T. et al. DAVID: a web server for functional enrichment analysis and functional annotation of gene lists (2021 update). *Nucleic Acids Res.* **50**, W216–221. https://doi.org/10.1093/nar/gkac194 (2022).

41. Kramer, A., Green, J., Pollard, J. Jr. & Tugendreich, S. Causal analysis approaches in ingenuity pathway analysis. *Bioinformatics* **30**, 523–530. https://doi.org/10.1093/bioinformatics/btt703 (2014).

Acknowledgements
Mass spectrometry-based proteomic analyses were performed by the Proteomics Core Facility, Department of Immunology, University of Oslo and Oslo University Hospital, which is supported by the Core Facilities program of the South-Eastern Norway Regional Health Authority. This core facility is also a member of the National Network of Advanced Proteomics Infrastructure (NAPI), which is funded by the Research Council of Norway INFRASTRUKTUR-program (project 295910). Transmission electron microscopy was performed by the core facility for Advanced Electron Microscopy Core Facility, Oslo University Hospital. We are thankful for all the patients and controls participating in our study and to all hospitals recruiting them.

Author contributions
AR and BAL take responsibility for the integrity of the study. Study conception and design: AR, FH, STF, BAL, RØ. Acquisition of samples and data: AR, STF, AMST, JG, MDM. Analysis and interpretation of data: AR, FH, TAN, STF, BAL, MS, JG, JE. Obtaining of funding: BAL, FH, MDM. All authors read and approved the final manuscript.

Competing interests
The authors declare no competing interests.

Additional information
Supplementary Information The online version contains supplementary material available at https://doi.org/10.1038/s41598-025-96325-8.

Correspondence and requests for materials should be addressed to A.R. or B.A.L.